Deep-Sea Research I 56 (2009) 32–40

Contents lists available at ScienceDirect

Deep-Sea Research I

journal homepage: www.elsevier.com/locate/dsri

Glimpses of Arctic Ocean shelf–basin interaction from submarine-borne radium sampling

David Kadko[a,*], Knut Aagaard[b]

[a] University of Miami, Rosenstiel School of Marine and Atmospheric Science, 4600 Rickenbacker Causeway, Miami, FL 33149, USA
[b] Polar Science Center, Applied Physics Laboratory, University of Washington, 1013 NE 40th Street, Seattle, WA 98105, USA

ARTICLE INFO

Article history:
Received 18 January 2008
Received in revised form
1 August 2008
Accepted 11 August 2008
Available online 20 August 2008

Keywords:
Arctic Ocean
Radium
Arctic shelves
Eddies

ABSTRACT

Evidence of shelf-water transfer from temperature, salinity, and $^{228}Ra/^{226}Ra$ sampling from the nuclear submarine *USS L. Mendel Rivers* SCICEX cruise in October, 2000 demonstrates the heterogeneity of the Arctic Ocean with respect to halocline ventilation. This likely reflects both time-dependent events on the shelves and the variety of dispersal mechanisms within the ocean, including boundary currents and eddies, at least one of which was sampled in this work. Halocline waters at the 132 m sampling depth in the interior Eurasian Basin are generally not well connected to the shelves, consonant with their ventilation within the deep basins, rather than on the shelves. In the western Arctic, steep gradients in $^{228}Ra/^{226}Ra$ ratio and age since shelf contact are consistent with very slow exchange between the Chukchi shelf and the interior Beaufort Gyre. These are the first radium measurements from a nuclear submarine.

1. Introduction

It is now over a century ago that Nansen (1902) recognized the extensive influence on the upper Arctic Ocean of the surrounding shelf seas. Sixty years later, seminal discussions by Coachman and Barnes (1961, 1962) of both the Pacific and Eurasian shelf influences on the Arctic Ocean, including summaries of Russian work during the intervening years, renewed widespread interest in the topic. The focus was subsequently sharpened by Aagaard et al. (1981), who argued the particular importance to the Arctic Ocean of its pronounced halocline and proposed shelf connections to that feature. Since then, numerous studies, and indeed whole research programs, have been dedicated to interactions between the Arctic Ocean and the adjacent shelves (for examples cf., Killworth and Smith, 1984; Jones and Anderson, 1986; Wallace et al., 1987; Rudels et al., 1996; Schauer et al., 1997; Steele and Boyd, 1998; Grebmeier and Harvey, 2005; Woodgate et al., 2005a).

Initially, attention was concentrated on the role of plumes in moving shelf waters offshore (Melling and Lewis, 1982), but later the interest shifted to other processes, including transfer along the continental margins and ridges by topographically constrained boundary currents (Aagaard, 1989), offshore fluxes forced by double-diffusive mechanisms (Carmack et al., 1997) or resulting from partial breakdown of the boundary currents (Smith et al., 1999), and eddies propagating into the interior from a baroclinically unstable boundary current (Pickart et al., 2005).

Here, we discuss such shelf-water transfer processes, using temperature, salinity, and radium isotope ratio ($^{228}Ra/^{226}Ra$) measurements from the nuclear submarine *USS L. Mendel Rivers* SCICEX accommodation cruise in October, 2000. The ^{228}Ra is derived from shelf sediments and is therefore a specific marker for waters that have resided on the shelves, and the use of the isotopic ratio

* Corresponding author. Tel.: +1 305 421 4721.
E-mail address: dkadko@rsmas.miami.edu (D. Kadko).

0967-0637/$ - see front matter
doi:10.1016/j.dsr.2008.08.002

precludes complications arising from possible biological or particle uptake of radium. Moreover, the half-life of ^{228}Ra (5.77 yr) is comparable to advective time scales within the Arctic Ocean, but much shorter than the half-life of ^{226}Ra (1620 yr), so that the isotopic ratio provides a useful estimate of the time elapsed since the waters left the shelf (e.g., Rutgers van de Loeff et al., 1995, 2003; Kadko and Muench, 2005; Kadko et al., 2008).

2. Methods

Unlike the earlier dedicated SCICEX scientific submarine cruises that included civilian scientists, accommodation cruises allow scientific sampling, but without civilian participation at sea (Arctic Ocean Science, SCICEX 2000 workshop report, 1999). Onboard biological and chemical analyses of water samples are therefore not possible, and water must be stored for later analysis ashore. Determination of dissolved oxygen, for example, is effectively eliminated.

To sample radium, approximately 130 l of seawater were collected from a hull intake port and filtered at $\sim$0.7 l min^{-1} through a manganese-coated acrylic fiber which adsorbs radium isotopes efficiently and without fractionation (Moore et al., 1985). The fibers were subsequently sealed in plastic petrie dishes and then counted ashore by gamma-spectrometry using established procedures (e.g., Michel et al., 1981; Rutgers van de Loeff et al., 1995, 2003; Kadko and Muench, 2005). The water draw and filtration occurred at a depth of 132 m while the submarine was underway, and typically each sample required $\sim$3 h and up to $\sim$90 km of cruise track.

Temperature and salinity were obtained from SeaBird SBE-19 CTDs mounted external to the hull near the top of the sail, 15 m above the keel. (Note that the seawater intake for the radium draw was approximately 14 m below the CTD.) The two SeaBirds were calibrated both pre- and post-cruise, and on that basis we judge them accurate to better than 0.01 °C and 0.01 in salinity. In addition, expendable CTDs (XCTDs) were launched from the submarine approximately every 30–45 km, depending on the location. These probes sampled from near-surface to $\sim$1000 m. The linear regression of a 20% sub-sample of the XCTD profiles, sampled at 118 m, with the corresponding SeaBird values yields an expected difference of $\sim$0.3 °C and 0.1 in salinity, with the XCTD sample being colder and fresher. The discrepancies are, respectively, about 10 and 5 times greater than the XCTD manufacturer's published accuracy. In contrast, comparison of ship-based SeaBird 911 data with XCTD casts in the same environment (Kadko et al., 2008) has shown agreement close to the published XCTD accuracy ($\sim$0.02 °C and $\sim$0.03 in salinity). Examination of individual CTD/XCTD data pairs, i.e., from the same time and location, suggests that the discrepancy is most pronounced in areas of large vertical gradients along the SCICEX track. Very likely, this reflects the inability of the sail-mounted CTDs to sample an undisturbed environment, but rather bias the measurements toward the deeper values intercepted by the hull, in this case warmer and more saline. In contrast, the XCTDs do not distort the temperature and salinity fields, but their accuracy is less. Faced with this dilemma, we have chosen to accept the XCTD profiles as correct, with accuracy limits approximately as specified by the manufacturer, consonant with the findings of Kadko et al. (2008). This does not have serious consequences for our analysis, since we primarily use the XCTD sections to examine features of the density field and the temperature and salinity of the water sampled for radium over approximately 90 km track segments (Table 1).

Although additional sensors (dissolved oxygen, transmissometer, and fluorometer) were mounted on the sail, all of these sensors failed before the start of data recording.

The sampling began in the northern Nansen Basin, extended across the Amundsen Basin and the Lomonosov Ridge, the northern Makarov and Canada basins, and the eastern Chukchi Borderland (CBL), thence westward over the Chukchi continental slope (Fig. 1). The trans-Arctic portion follows the 1998 and 1999 SCICEX tracks between 85°N, 46°E and 72.5°N, 155.75°W. This track segment was conducted as a straight, continuous transect, and the radium samples reported here were from 132 m depth. The track segment midpoint for each radium filtration is shown in Fig. 1 along with the measured ^{228}Ra/^{226}Ra ratio.

3. Results

The results are listed in Table 1. The salinity distribution in the upper 300 m (Fig. 2) reflects the relatively saline upper waters on the Eurasian side of the Arctic Ocean (Schauer et al., 2002) grading into the large freshwater storage of the upper Canada Basin (Aagaard and Carmack, 1989), with the isohalines rising again over the Beaufort slope (Aagaard, 1984; Pickart, 2004), indicative of the Pacific water influence upon flows along the basin boundary.

3.1. Rapid eddy transfer

By far the highest ^{228}Ra/^{226}Ra ratio observed in the section is the value 1.60 found near the southeast flank of the Northwind Ridge in the Canada Basin (Fig. 1; sample 26, Table 1), representing water that has been in recent contact with shelf sediments. The density distribution along this portion of the section (Fig. 3) shows that a portion of the radium sample was taken within the upper half of an anti-cyclonic eddy that extended downward from the bottom of the mixed layer to almost 400 m. The eddy radius was no larger than the separation of the XCTD casts, about 44 km, and probably considerably less, since halocline eddies typically have a diameter of 30 km or less (e.g., Muench et al., 2000). The thermal wind velocity maximum was near 200 m, where the isopycnal slope changes sign with depth. Water properties at 200 m in the eddy core were near −1.8 °C and 33.65 in salinity, corresponding to a potential density of 1027.08 kg m^{-3}. The observed eddy core is identical in temperature to those found by Muench et al. 2000 and Pickart et al. 2005 for cold-core halocline eddies, but more saline by $\sim$0.4

Table 1
Radium analyses

Sample	Date collected	Depth (m)	$^{228}Ra/^{226}Ra$	Salinity[a]	Pot. temp[a] (°C)	Latitude north+	Longitude east+
1	10/17/2000	132	0.14 ± 0.03	34.51	−0.06	85.5	47.383
2	10/17/2000	132	0.14 ± 0.06	34.41	−0.40	86.08	50.533
3	10/17/2000	132	0.19 ± 0.14	34.34	−0.77	86.55	54.236
4	10/17/2000	132	0.13 ± 0.04	34.37	−0.73	87.22	60.25
5	10/18/2000	132	0.03 ± 0.39	34.29	−0.91	88.03	75.167
6	10/18/2000	132	0.56 ± 0.19	34.26	−1.35	88.38	91.767
7	10/18/2000	132	0.17 ± 0.04	34.34	−1.09	88.53	126.433
8	10/18/2000	132	0.09 ± 0.07	34.27	−1.38	88.25	152.783
9	10/18/2000	132	0.14 ± 0.15	34.10	−1.46	87.72	169.433
10	10/18/2000	132	0.28 ± 0.14	34.18	−1.24	87.17	179
11	10/18/2000	132	0.28 ± 0.06	34.33	−1.10	86.47	−175.07
12	10/19/2000	132	0.26 ± 0.02	34.33	−1.03	85.8	−171.15
13	10/19/2000	132	0.39 ± 0.08	34.15	−1.35	85.17	−168.45
14	10/20/2000	132	0.17 ± 0.07	34.03	−1.65	84.42	−166.0
15	10/20/2000	132	0.28 ± 0.13	33.86	−1.72	83.32	−163.67
16	10/20/2000	132	0.27 ± 0.34	33.81	−1.72	82.63	−162.47
17	10/20/2000	132	0.47 ± 0.08	33.87	−1.71	81.83	−161.35
18	10/20/2000	132	0.26 ± 0.04	33.88	−1.71	81.0	−160.5
19	10/20/2000	132	0.28 ± 0.01	33.87	−1.71	80.3	−159.85
20	10/20/2000	132	0.46 ± 0.01	33.77	−1.66	79.5	−159.25
22	10/21/2000	132	0.63 ± 0.03	33.15	−1.61	78.0	−158.25
23	10/21/2000	132	0.52 ± 0.01	32.89	−1.46	77.27	−157.78
24	10/21/2000	132	0.43 ± 0.06	32.74	−1.49	76.43	−157.36
25	10/21/2000	132	0.33 ± 0.03	32.77	−1.46	75.67	−157.05
26	10/21/2000	132[b]	1.60 ± 0.13	32.75	−1.47	74.83	−156.72
27	10/22/2000	132	0.35 ± 0.04	33.10	−1.51	74.18	−156.58
28	10/22/2000	132	0.40 ± 0.07	32.82	−1.48	73.42	−156.4
29	10/22/2000	132	0.65 ± 0.04	33.40	−1.45	72.67	−156.35
30	10/22/2000	132	0.91 ± 0.22	33.68	−1.51	72.53	−157.0
31	10/22/2000	132	0.74 ± 0.09	33.32	−1.41	72.77	−158.33
32	10/22/2000	132	0.48 ± 0.05	32.85	−1.49	72.22	−158.4
33	10/22/2000	132	0.49 ± 0.05	nd	nd	73.58	−160.33
34	10/22/2000	132	0.76 ± 0.03	nd	nd	73.92	−162.833
35	10/23/2000	132	0.72 ± 0.11	nd	nd	74.2	−165.77
36	10/23/2000	132	0.57 ± 0.05	33.3	−1.59	74.42	−168.67
37	10/23/2000	132	0.61 ± 0.07	33.45	−1.53	74.88	−169.72
38	10/23/2000	132	0.68 ± 0.03	33.64	−1.23	75.42	−170.53
39	10/23/2000	132	0.62 ± 0.08	33.4	−1.53	75.7	−172.33
40	10/23/2000	132	0.56 ± 0.06	nd	nd	75.75	−174.83
41	10/24/2000	132	0.60 ± 0.09	nd	nd	75.7	178.83
42	10/24/2000	132	0.37 ± 0.06	33.79	−1.33	75.83	177.85
43	10/24/2000	132	0.51 ± 0.06	33.68	−1.35	76.08	179.33
44	10/24/2000	132	0.63 ± 0.05	nd	nd	75.8	−177.917
45	10/24/2000	132	0.67 ± 0.06	33.50	−1.35	75.47	−175.33
46	10/24/2000	132	0.66 ± 0.03	33.79	−1.23	75.2	−175.37

[a] Mean values from local profiles taken over the spatially extensive Ra sampling. nd-not determined.
[b] Some shallower water sampled (see text).

than the mid-range they report. Farther south in the SCICEX section, over the upper Alaskan slope, this isopycnal was found 50–75 m higher in the water column and was ~0.6 °C warmer. The implication is that the eddy core water acquired its properties on the shelf during freezing and descended some 150 m as it moved offshore during the following spring and summer. This timescale is consistent with the radium isotope analysis (cf., below).

It is likely that the measured $^{228}Ra/^{226}Ra$ ratio of 1.6 is an underestimate, for contrary to standard practice on the cruise, sampling was not terminated when the submarine left its cruise depth and rose to the surface. Instead, the sampling continued during the entire ascent, contributing ~30% of the total sample volume. Data from two slope transects in the same area from 2002 and 2004 show that seaward of the slope the radium isotope ratio typically decreases markedly above 50–100 m (Kadko et al., 2008), so that our 2000 sample extending to the surface is likely biased toward a value lower than would have been obtained had the sampling all been done at the cruise depth as the eddy center was approached. The likelihood that the actual $^{228}Ra/^{226}Ra$ ratio at depth exceeded 1.60 makes the anomalous water properties even more pronounced and suggests a very recent connection of the eddy with shelf sediments.

Given typical radium isotope ratios over the western Arctic shelves, the ratio observed within the eddy can be used to estimate the time elapsed since the eddy waters were in contact with shelf sediments. This time T follows from the radioactive decay equation:

$$T = -\ln[R/R_0]\lambda, \quad (1)$$

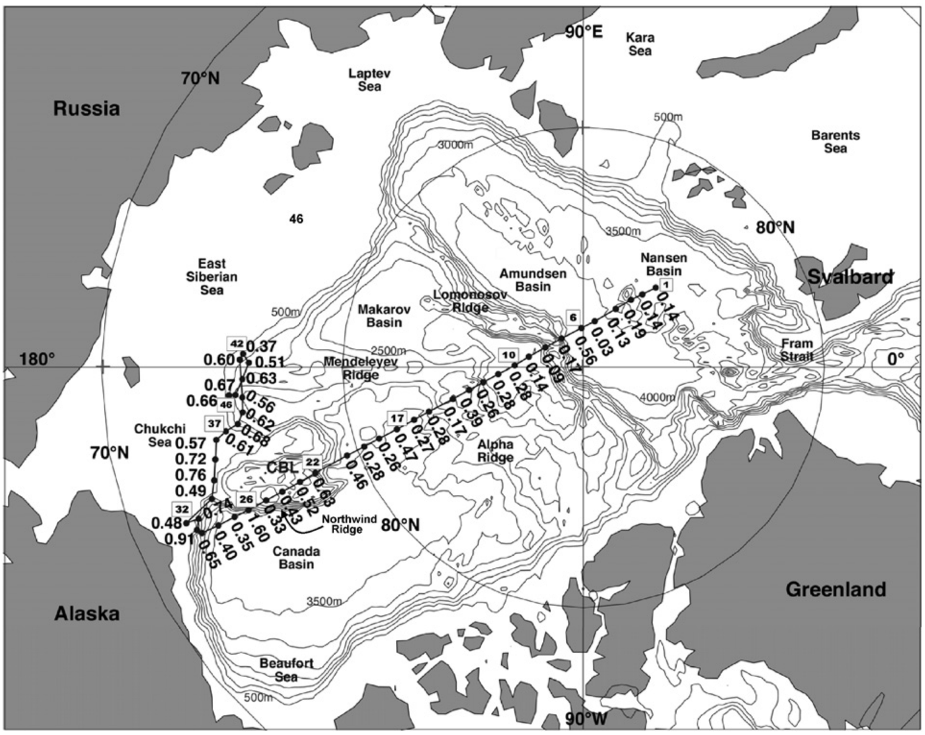

Fig. 1. SCICEX 2000 cruise track and observed radium ($^{228}Ra/^{226}Ra$) ratios. Selected sample numbers are indicated by boxed numbers. The Nansen and Amundsen basins together constitute the Eurasian Basin, and the Makarov and Canada basins the Canadian Basin. CBL signifies the Chukchi Borderland.

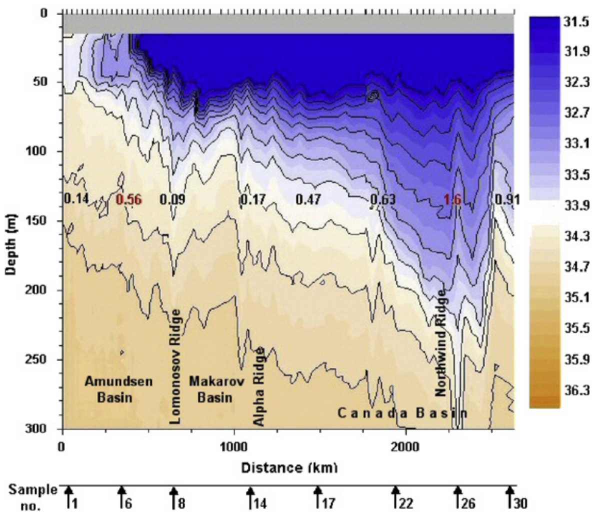

Fig. 2. Salinity along the trans-Arctic portion of the SCICEX 2000 section, based on XCTD casts. Location of the XCTD casts are indicated by upper tick marks. Selected $^{228}Ra/^{226}Ra$ ratios (Fig. 1, Table 1) are also shown. Two of these, corresponding to anomalously high values discussed in the text, are highlighted in red. Several bathymetric features are noted.

where λ is the decay constant of ^{228}Ra ($0.12\,yr^{-1}$), R the observed $^{228}Ra/^{226}Ra$ ratio, and R_0 the initial $^{228}Ra/^{226}Ra$ ratio prior to leaving the shelf.

Kadko and Muench (2005) derived a $^{228}Ra/^{226}Ra$ approximation for zero-age water coming off the Beaufort–Chukchi shelf: $R_0 = -0.486\ S+17.25$, where S is the salinity. This approximation yields a radium isotope ratio of 1.33 for sample 26, indistinguishable from the observed ratio $R = 1.60 \pm 0.13$ for $S = 32.75$ (Table 1). Considering the half-life of the isotope (5.77 yr), this suggests that within the errors of the approximation and measurement, the water had only recently (months, i.e., the previous winter or spring) been in contact with shelf sediments.

The vertical extent of this cold eddy, as well as its water properties, are remarkably similar to those described by Muench et al. (2000) for an anticyclone observed in the same region and about the same distance from the shelf. Based in part on the calculated tritium–helium age, Muench et al. (2000) suggested that their feature was over a year old, requiring a mean translational speed of $\sim 0.01\,m\,s^{-1}$ from the shelf. Pickart et al. (2005) have recently suggested that this age could be an overestimate, however, because of incomplete atmospheric equilibration of the tracer. Although our own eddy was found at the base of the steep western flank of the Northwind Ridge, consonant with southward advection along the ridge by a boundary current circumnavigating the CBL (Woodgate et al., 2007), the very recent contact of the core waters with the shelf argues against the eddy following this long route. Rather, the eddy likely entered the southwest Canada Basin directly from the Chukchi shelf (Pickart et al., 2005; Kadko et al., 2008), a route that we discuss further below. In this connection, we note that summer data presented in Kadko et al. (2008, their Fig. 9) indicate offshore patchiness in this region, both for temperature and radium isotope ratio, suggestive of eddies derived from the boundary current.

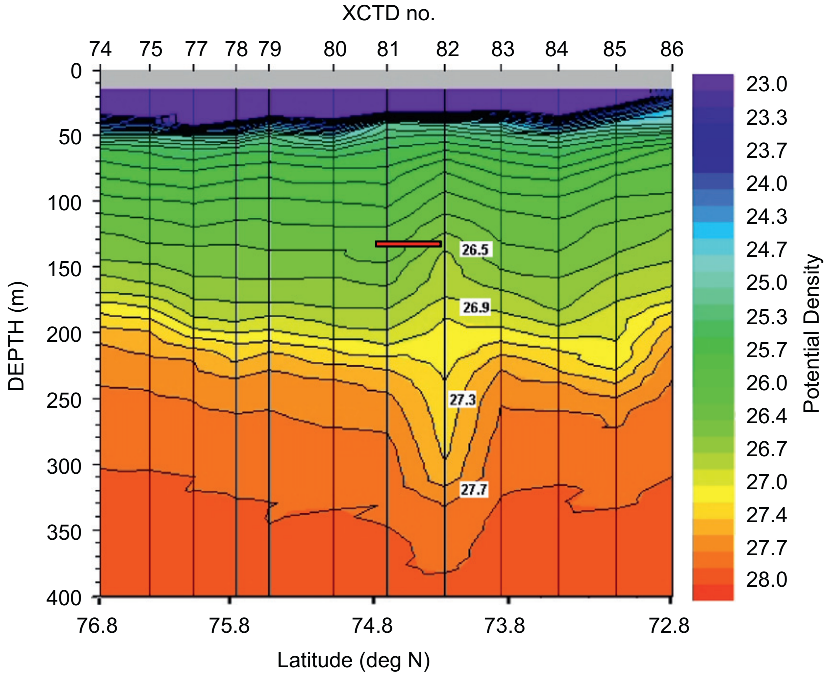

Fig. 3. Isopycnals in the portion of the trans-Arctic section that includes the eddy associated with radium sample 26. The red horizontal bar indicates the approximate location of the sample. Right-hand color scale is potential density in sigma notation.

3.2. Other, slower transfers

The $^{228}Ra/^{226}Ra$ ratios observed in the section extending northwestward over the Chukchi slope are in general elevated above those in the trans-Arctic section (Fig. 1), and are similar to those found by Kadko and Muench (2005) (May–June 2002) and Kadko et al. (2008) (July–August 2002 and 2004) at comparable locations and depths. For example, for stations between the 500 and 2000 m isobaths, the cited radium isotope ratios range from 0.23–1.08 at depths between 100 and 165 m, while ours are 0.37–0.91 at the constant 132 m sampling depth. Furthermore, the cited samples are from spring and summer, while ours are from mid-late October, suggesting that there is no obvious seasonal variability in the offshore flux of shelf water, or at least not in the amount of shelf-water retained over the slope, even though the boundary current described by Nikolopoulos et al. (in press) shows marked seasonal differences.

In the trans-Arctic section, several samples exhibit $^{228}Ra/^{226}Ra$ ratios considerably higher than those over most of the deep basins, but comparable to those seen over the slope. The first of these (sample 6, Table 1; Fig. 4) was taken over the abyssal plain of the Amundsen Basin at 90°E (Fig. 1), where the sample $^{228}Ra/^{226}Ra$ ratio of 0.56 greatly exceeds any other ratio from this basin (0.03–0.19), pointing to a shelf connection. The temperature and salinity at 132 m from the XCTD profiles that bracket sample 6 are, respectively, −1.1 to −1.3 °C and 34.3 (Fig. 4, top). Nearby stations from 1991 *Oden* cruise (Anderson et al., 1994) show a similar salinity at this depth, but the *Oden* water is warmer by ~0.2 °C. Stations in the southern Nansen Basin from 1995 *Polarstern* cruise (Rudels et al., 2000) show that water of the same salinity as our samples, but colder by 0.2–0.6 °C, effectively outcrops near the Kara and Laptev shelf breaks, being found within 30–50 m of the sea surface. We therefore assume that the enhanced radium isotope ratio of sample 6 represents a shelf contribution from either the Laptev or Kara seas, and that it has retained some of its original low temperature. Taking the Laptev shelf as the closest possible source, places it ~1100 km upstream along the Eurasian Basin boundary from where the SCICEX 2000 cruise track ascends the Lomonosov Ridge flank. The translational speed along the Eurasian flank of the ridge is ~2 cm s^{-1} (Swift et al., 1997; Woodgate et al., 2001), giving an advective time scale of just under 2 yr. Moving the water southward from the ridge flank to the sample location will add to this estimate. These considerations suggest that the water represented by sample 6 is no less than two years from its Eurasian shelf source, but that other samples along the SCICEX track crossing the Eurasian Basin are far more removed in time from the shelf.

Earlier radium data (Rutgers van de Loeff et al., 1995) indicated that the advective time scale of near-surface waters carried from the eastern Arctic shelves toward Fram Strait by the Transpolar Drift is <3 yr, but with large uncertainty. More detailed data from the Siberian shelves (Rutgers van de Loeff et al., 2003) suggest that the ^{228}Ra signal derived from the Laptev Sea can be considered as representative of joint input from both the Kara and Laptev shelves. The mean radium isotope ratio over these shelves for a salinity comparable to that of our sample 6 is ~0.65 (although one shelf sample taken near the seafloor showed a ratio of 1.64). From Eq. (1), with $R_0 = 0.65$ and

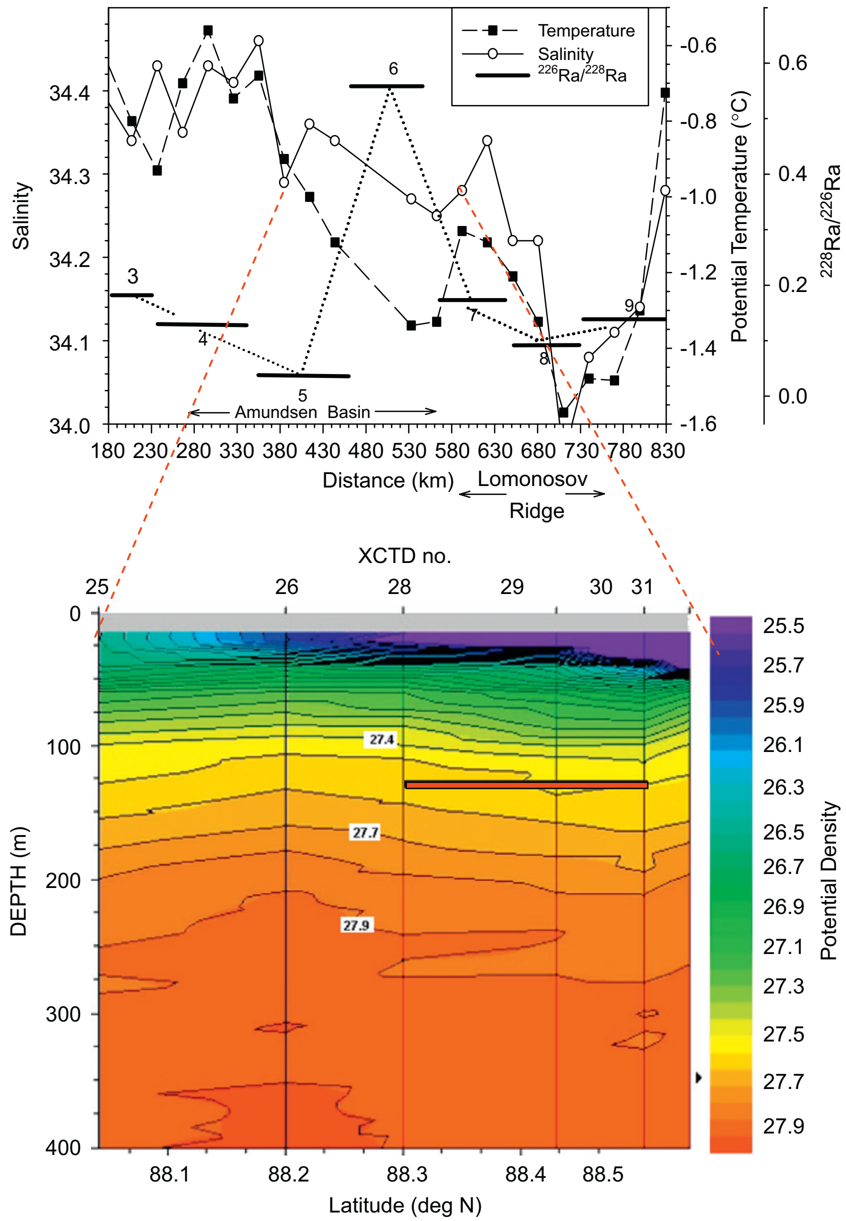

Fig. 4. (Top): $^{228}Ra/^{226}Ra$ ratio, temperature, and salinity at 132 m in the trans-Arctic section segment represented by Ra samples 3–9 (numbered). Temperature and salinity are from the XCTD casts. The anomalously high radium isotope ratio and low temperature of sample 6 likely represent a Eurasian shelf contribution. The radium samples, collected underway, cover up to ~90 km of cruise track. (Bottom): Isopycnals in the portion of the trans-Arctic section that includes radium sample 6. The red horizontal bar indicates the approximate location of the sample. Right-hand color scale is potential density in sigma notation.

$R = 0.56 \pm 0.19$, the elapsed time T is in the range 0–4.7 yr, with our estimated advective time scale of 2+ yr falling in the middle of this range. In contrast, the adjacent low-ratio samples of similar salinity would not have had contact with the shelf environment for at least 10–25 yr.

While our hypothesis that the shelf-derived water of sample 6 was carried with the boundary current along the margin of the Nansen and Amundsen basins appears reasonable, there are few clues to the manner of its detachment from the Lomonosov Ridge flank and drift into the interior. In particular, the XCTD casts (Fig. 4, bottom) show no indication of an eddy. However, halocline eddies in the Arctic Ocean are typically 10–20 km in diameter (e.g., Manley and Hunkins, 1985; Muench et. al., 2000; Mathis et al., 2007), while the separation of the XCTD casts shown in Fig. 4 is about 30 km. The sampling interval is therefore insufficient to define an eddy unambiguously, or even to detect it unless one of the casts sectioned it, as was the case for the eddy described earlier in connection with radium sample 26 (Fig. 3). Long-term moored measurements ~100 km away over the abyssal plain show eddies to be common, including in the halocline (Aagaard et al., 2008). In this connection, we note that the locally reduced temperature and salinity in the portion of the cruise track covered by radium sample 6 could conceivably be influenced by a cold-core eddy, even if the density field is not sufficiently resolved to show the eddy itself.

The low $^{228}Ra/^{226}Ra$ ratios prevailing along the trans-Arctic section across the Nansen and Amundsen basins continue into the northern Makarov Basin (sample 9), suggesting at least a temporal kinship that extends across the Lomonosov Ridge. The low radium isotope ratios, typically <0.2 in this area (Rutgers van de Loeff et al., 1995), and high salinity marking the saline Atlantic inflow through Fram Strait indicate that there is little interaction with shelves. Farther south in the Canadian Basin, however, where salinity decreases, the $^{228}Ra/^{226}Ra$ ratio increases, and between the northern Makarov Basin and the CBL they are, with one exception (sample 14), within the range 0.26–0.47, corresponding to a closer connection with the shelf seas. This connection is with the Eurasian shelves, however, not with the Chukchi shelf and its Pacific waters. This is clear from the temperature and salinity of the samples, $<-1.7\,°C$ and 33.8–33.9, respectively. These values are typical for the Eurasian and Makarov basins, where water with such characteristics is found above 100 m (Anderson, et al., 1994; Swift et al., 1997). In contrast, even the coldest halocline waters in the Arctic Ocean of Pacific origin are fresher (Coachman and Barnes, 1961; Swift et al., 1997). This portion of the 2000 SCICEX section therefore demonstrates the pervasive influence of the Eurasian shelves in parts of the Arctic Ocean halocline that at other times have been dominated by a Pacific source, including the northwestern Canada Basin (compare McLaughlin et al., 1996; Swift et al., 2005).

Apart from the eddy discussed above (sample 26), the highest $^{228}Ra/^{226}Ra$ ratios found north of the Beaufort slope are clustered in samples 22–23 (Fig. 5, Table 1), over the northeastern portion of the CBL (Fig. 1). The salinity of these samples (32.89–33.15) closely brackets that of the halocline mode induced by the Pacific inflow to the Arctic Ocean (Aagaard and Carmack, 1989). Based on the radium isotope ratio, the time elapsed since the water was in contact with the shelf sediments is 5–7 yr (Fig. 5). There are two possible routes from the Chukchi shelf to the observed location. One route follows the slope contours clockwise around the CBL (Woodgate et al., 2007). Along this path, the distance from the 100 m isobath in the northwestern Chukchi Sea, which is the discharge point of the northward flow of Pacific waters through Herald Canyon (Weingartner et al., 2005; Woodgate et al., 2005b), thence following the steepest topography northward and eastward around the CBL to the locations of our samples 22–23, is ~1300 km. Woodgate et al. (2007) have estimated the mean speed of the Atlantic layer along this general route to be 1–2 cm s^{-1}, which if applied to the halocline layer yields an advective time scale of 2–4 yr, about half that indicated by the $^{228}Ra/^{226}Ra$ ratio. Regardless of this discrepancy, which cannot be resolved absent independent halocline advection rate estimates over this route, it appears likely that the dispersal of Pacific shelf waters into the interior Arctic Ocean via the anti-cyclonic CBL pathway requires several years at a minimum.

The second possible route from the Chukchi shelf to the northeastern CBL is northward along the Northwind Ridge, which forms the steep eastern flank of the CBL (Fig. 1). (Shimada et al., 2001 and Spall et al., in press) have argued that a northward baroclinic flow over this ridge, along the western margin of the wind-driven Beaufort Gyre, provides direct access for shelf waters from the Chukchi into the interior Canada Basin. If so, this would be a likely route for the eddy discussed in connection with sample 26, representing very recent contact with the shelf. The direct distance of that sample location from the shelf is ~100 km, which could be traversed in 2 months (cf., earlier discussion) by a mean flow of 2 cm s^{-1}. If this Northwind Ridge route is the one taken by the waters represented by radium samples 22–23, then why is the indicated elapsed time since shelf contact (5–7 yr), so much longer than that of the eddy? One possibility is that

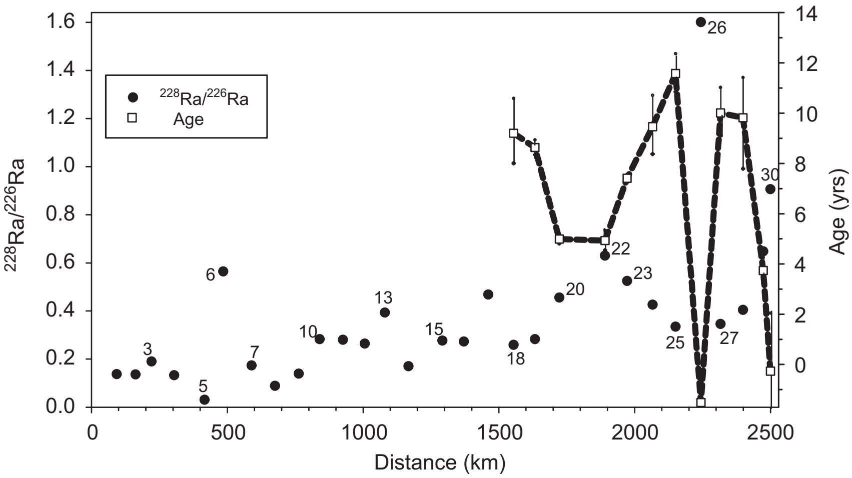

Fig. 5. Radium isotope ratio along the trans-Arctic section together with elapsed time since contact with the Pacific shelf, based on the method of Kadko and Muench (2005) (cf., text). Within the initial value approximation and the 5.77 yr half-life of ^{228}Ra, negative ages are indistinguishable from zero.

since the other samples are not from the ridge flank, but from the plateau to the west of the ridge, they reflect a far more stagnant regime (compare Woodgate et al., 2007).

Finally, we note the sharp increase in radium isotope ratio approaching the continental slope (samples 28–30), with a corresponding age difference across the slope of ~10 yr (Fig. 5). This has also been noted in earlier work where it was suggested that steep gradients in $^{228}Ra/^{226}Ra$ ratio and age are consistent with very slow exchange between the Chukchi shelf and the interior Beaufort gyre (Hansell et al., 2004; Kadko and Muench, 2005). These investigators have argued that the low radium isotope ratios, low salinity and low $\delta^{18}O$ found offshore in the Beaufort gyre are indicative of re-circulated, aged river water that is isolated from shelf interaction.

4. Discussion

Two over-riding issues are particularly worthy of attention. First, the radium measurements demonstrate the heterogeneity of the Arctic Ocean with respect to shelf ventilation: the $^{228}Ra/^{226}Ra$ ratio (age since shelf ventilation) in the interior ocean is distinctly patchy (Fig. 5). This may in part result from time-dependent events on the shelves, e.g., formation of dense, saline water in wind-driven coastal polynyas, which have typical time scales of a few days to a week or more (Danielson et al., 2006). Alternatively, the heterogeneity in the interior may arise from episodic shelf outflows with a time scale that is governed by shelf edge dynamics, e.g., eddy formation, downwelling, or plume discharge. Indeed, the growing evidence for an abundance of eddies within the Arctic Ocean, carrying waters with shelf or slope characteristics (such as our radium sample 26), speaks to the importance of instabilities along the basin margins. The boundary currents that overlie these margins play a large and distinctive role in dispersing shelf waters and ventilating the halocline, a role that goes beyond simply shedding eddies. In particular, these topographically steered flows provide efficient long-range transport along the basin margins, as was the case for our radium sample 6. At the same time, the boundary flows are also leaky, in the sense that they discharge a portion of their burden into the interior. Depending on stratification and slope topography, that leakiness may vary in both time and location. While much of the discharge into the interior likely does involve eddy shedding by a baroclinically unstable boundary flow (cf., Spall et al., in press for a recent discussion), there are other plausible sources of leakiness. For example, the remarkable basin-scale coherence of the temperature–salinity fine structure in the Arctic Ocean (Carmack et al., 1997), points toward fluxes from the boundary current that are forced by double-diffusion (Walsh and Carmack, 2002, 2003). In other cases, flow separation induced by margin topography may drive transfers into the interior. We suggest that a variety of mechanisms is responsible for the patchy interior ventilation indicated by the radium measurements.

The second over-riding issue is addressed by the very low $^{228}Ra/^{226}Ra$ ratios we find over the first 700 km or so of the trans-Arctic section, across the Nansen and Amundsen basins and into the northern Makarov Basin. These ratios suggest that the halocline waters sampled along this route are not recently or well connected with the shelves. The poor communication with the shelf does not necessarily mean that this layer is poorly ventilated, but rather that for effective halocline renewal, other ventilating sources are likely more important. Itoh et al. (2007) have recently examined a large composite data set to test the early suggestion of Rudels et al. (1996) that the halocline waters in these basins are being renewed from the surface, rather than from the Eurasian shelves. Itoh et al. (2007) find compelling evidence for such renewal by surface-driven winter convection within the southwestern Nansen Basin, with the ventilated waters subsequently spreading laterally into both the Amundsen and Makarov basins. The convective renewal appears centered on the portion of the lower halocline demarked by $34.1 < S < 34.3$, which is cold, relatively well oxygenated, and of low potential vorticity. Their view is not incompatible with the analysis of the upper Arctic Ocean oxygen distribution by Falkner et al. (2005), who emphasize the low-oxygen contributions to the halocline from the western Arctic shelves, contributions that lead to a complex oxygen field with intermediate maxima.

Almost 30 yr have passed since Aagaard et al. (1981) advanced their greatly simplified model of shelf ventilation of the halocline. It is now clear that the Arctic Ocean halocline, so very important to the upper ocean and its winter ice cover, is a feature complicated in both time and space. There are numerous connections to the shelves, but there are also other sources of ventilation, particularly on the Eurasian side of the ocean. How these various connections and sources will evolve as the Arctic Ocean responds to the earth's changing climate is a matter of considerable concern and interest.

Acknowledgements

We are indebted to the crew of the *USS L. Mendel Rivers* for their contribution to the collection of these data through precise submarine operation in a challenging environment. We particularly thank Petty Officers S. Baker, C. Crook, C. Meadows, and R. Sarwal for their water sampling efforts. The field work was facilitated by J. Gossett of the Arctic Submarine Laboratory. We thank Dr. R. Pickart and an anonymous reviewer for their helpful comments. Our efforts were supported by NSF grants OCE-9809168 and OPP-9701067 (DK) and OPP 0352754 (KA).

References

Aagaard, K., 1984. The beaufort undercurrent. In: Barnes, P., Reimnitz, E. (Eds.), The Alaskan Beaufort Sea: Ecosystems and Environment. Academic Press, New York, pp. 47–71.

Aagaard, K., 1989. A synthesis of the Arctic Ocean circulation. Rapp. P.-V. Reun. Conservation and international Exploration Mer. 188, 11–22.

Aagaard, K., Carmack, E.C., 1989. The role of sea ice and other fresh water in the arctic circulation. Journal of Geophysical Research 94, 14,485–14,498.

Aagaard, K., Coachman, L.K., Carmack, E.C., 1981. On the halocline of the Arctic Ocean. Deep-Sea Research 28, 529–545.

Aagaard, K., Andersen, R., Swift, J., Johnson, J., 2008. A large eddy in the central Arctic Ocean. Geophysical Research Letters 35, L09601.
Anderson, L.G., Björk, G., Holby, O., Jones, E.P., Kattner, G., Koltermann, K.P., Liljeblad, B., Lindegren, R., Rudels, B., Swift, J., 1994. Water masses and circulation in the Eurasian Basin: results from the *Oden* 91 expedition. Journal of Geophysical Research 99, 3273–3283.
Arctic Ocean Science from Submarines—A report based on the SCICEX 2000 Workshop, Warrenton, Virginia 5–9 October, 1998 (1999), SCICEX 2000 Workshop Organizing Committee: D. Rothrock and W. Maslowski (co-chairs), Applied Physics Laboratory, University of Washington.
Carmack, E.C., Aagaard, K., Swift, J.H., Macdonald, R.W., McLaughlin, F.A., Jones, E.P., Perkin, R.G., Smith, J.N., Ellis, K., Kilius, L., 1997. Changes in temperature and contaminant distributions within the Arctic Ocean. Deep-Sea Research Part II 44, 1487–1502.
Coachman, L.K., Barnes, C.A., 1961. The contribution of Bering sea water to the Arctic Ocean. Arctic 14, 146–161.
Coachman, L.K., Barnes, C.A., 1962. Surface water in the Eurasian Basin of the Arctic Ocean. Arctic 15, 251–277.
Danielson, S., Aagaard, K., Weingartner, T., Martin, S., Winsor, P., Gawarkiewicz, G., Quadfasel, D., 2006. The St. Lawrence polynya and the Bering shelf circulation: new observations that test the models. Journal of Geophysical Research 111, C09023.
Falkner, K.K., Steele, M., Woodgate, R.A., Swift, J.H., Aagaard, K., Morison, J., 2005. Dissolved oxygen extrema in the Arctic Ocean halocline from the North Pole to the Lincoln Sea. Deep-Sea Research I 52, 1138–1154.
Grebmeier, J.M., Harvey, H.R., 2005. The western Arctic shelf-basin interactions (SBI) project: an overview. Deep-Sea Research II 52, 3109–3115.
Hansell, D.A., Kadko, D., Bates, N.R., 2004. Non-conservative behavior of terrigenous dissolved organic carbon in the western Arctic Ocean. Science 304, 858–861.
Itoh, M., Carmack, E., Shimada, K., McLaughlin, F., Nishino, S., Zimmermann, S., 2007. Formation and spreading of Eurasian source oxygen-rich halocline water into the Canadian Basin of the Arctic Ocean. Geophysical Research Letters 34, L08603, 10.1029/2007GL029482.
Jones, E.P., Anderson, L.G., 1986. On the origin of the chemical properties of the Arctic Ocean halocline. Journal of Geophysical Research 91, 10,759–10,767.
Kadko, D., Muench, R., 2005. Evaluation of shelf-basin interaction in the western Arctic by use of short-lived radium isotopes: the importance of mesoscale processes. Deep-Sea Research II 52, 3227–3244.
Kadko, D., Pickart, R., Mathis, J., 2008. Age characteristics of a shelf-break eddy in the western Arctic and implications for shelf-basin exchange. Journal of Geophysical Research 113, C02018, 10.1029/2007JC004429.
Killworth, P.D., Smith, J.M., 1984. A one-and-a-half dimensional model for the Arctic halocline. Deep-Sea Research 31, 271–293.
Manley, T.O., Hunkins, K., 1985. Mesoscale eddies of the Arctic Ocean. Journal of Geophysical Research 90, 4911–4930.
Mathis, J.T., Pickart, R.S., Hansell, D.A., Kadko, D., Bates, N.R., 2007. Eddy transport of organic carbon and nutrients from the Chukchi shelf: impact on the upper halocline of the western Arctic Ocean. Journal of Geophysical Research 112, C05011, 10.1029/2006JC003899.
McLaughlin, F., Carmack, E., Macdonald, R., Bishop, J., 1996. Physical and geochemical properties across the Atlantic/Pacific water mass boundary in the southern Canadian Basin. Journal of Geophysical Research 101, 1193–1198.
Melling, H., Lewis, E.L., 1982. Shelf drainage flows in the Beaufort Sea and their effect on the Arctic Ocean pycnocline. Deep-Sea Research, Part A 29, 967–985.
Michel, J., Moore, W.S., King, P.T., 1981. γ-Ray spectrometry for determination of radium-228 and radium-226 in natural waters. Analytical Chemistry 53, 1885–1889.
Moore, W.S., Key, R.M., Sarmiento, J.L., 1985. Techniques for precise mapping of ^{226}Ra and ^{228}Ra in the ocean. Journal of Geophysical Research 90, 6983–6994.
Muench, R.D., Gunn, J.T., Whitledge, T.E., Schlosser, P., Smethie Jr., W.S., 2000. An Arctic Ocean cold-core eddy. Journal of Geophysical Research 105, 23,997–24,006.
Nansen, F., 1902. Oceanography of the north polar Basin. Scientific Results of the Norwegian North Polar Expedition 1893–96 III (9), 427.
Nikolopoulos, A., Pickart, R.S., Fratantoni, P.S., Shimada, K., Torres, D.J., Jones, E.P., (in press). The western Arctic boundary current at 152 W: Structure, variability, and transport, Deep-Sea Research II.
Pickart, R.S., 2004. Shelfbreak circulation in the Alaskan Beaufort Sea: mean structure and variability. Journal of Geophysical Research 109, C04024.
Pickart, R.S., Weingartner, T.J., Pratt, L.J., Zimmermann, S., Torres, D.J., 2005. Flow of winter-transformed Pacific water into the western Arctic. Deep-Sea Research II 52, 3175–3198.
Rudels, B., Anderson, L.G., Jones, E.P., 1996. Formation and evolution of the surface mixed layer and halocline of the Arctic Ocean. Journal of Geophysical Research 101, 8807–8821.
Rudels, B., Muench, R.D., Gunn, J., Schauer, U., Friedrich, H.J., 2000. Evolution of the Arctic Ocean boundary current north of the Siberian shelves. Journal of Marine systems 25, 77–99.
Rutgers van der Loeff, M.M., Key, R.M., Scholten, J., Bauch, D., Michel, A., 1995. ^{228}Ra as a tracer for shelf water in the Arctic Ocean. Deep-Sea Research II 42, 1533–1553.
Rutgers van der Loeff, M., Kuhne, S., Wahsner, M., Holtzen, H., Frank, M., Ekwurzel, B., Mensch, M., Rachold, V., 2003. ^{228}Ra and ^{226}Ra in the Kara and Laptev seas. Continental Shelf Research 23, 113–124.
Schauer, U., Muench, R.D., Rudels, B., Timokhov, L., 1997. Impact of eastern Arctic shelf waters on the Nansen Basin intermediate layers. Journal of Geophysical Research 102, 3371–3382.
Schauer, U., Rudels, B., Jones, E.P., Anderson, L.G., Muench, R.D., Bjørk, G., Swift, J.H., Ivanov, Larsson, A.-M., 2002. Confluence and redistribution of Atlantic water in the Nansen, Amundsen and Makarov basins. Annales Geophysicae 20, 257–273.
Shimada, K., Carmack, E.C., Hatakeyama, K., Takizawa, T., 2001. Varieties of shallow temperature maximum waters in the western Canadian Basin of the Arctic Ocean. Journal of Geophysical Research 28 (18), 3441–3444.
Smith, J.N., Ellis, K.M., Boyd, T., 1999. Circulation features in the central Arctic Ocean revealed by nuclear fuel reprocessing tracers from scientific ice expeditions 1995 and 1996. Journal of Geophysical Research 104, 29,663–29,677.
Spall, M.A., Pickart, R.S., Fratantoni, P.S., Plueddemann, A.J., 2008. Western Arctic shelfbreak eddies: Formation and transport. Journal of Physical Oceanography 38, 1644–1668.
Steele, M., Boyd, T., 1998. Retreat of the cold halocline layer in the Arctic Ocean. Journal of Geophysical Research 103, 10,419–10,435.
Swift, J.H., Jones, E.P., Aagaard, K., Carmack, E.C., Hingston, M., Macdonald, R.W., McLaughlin, F.A., Perkin, R.G., 1997. Waters of the Makarov and Canada basins. Deep-Sea Research Part II 44, 1503–1529.
Swift, J.H., Aagaard, K., Timokhov, L., Nikiforov, E.G., 2005. Long-term variability of Arctic Ocean waters: evidence from a reanalysis of the EWG data set. Journal of Geophysical Research 110 (C3), C03012.
Wallace, D.W., Moore, R.M., Jones, E.P., 1987. Ventilation of the Arctic Ocean cold halocline: rates of diapycnal and isopycnal transport, oxygen utilization, and primary production inferred using chlorofluormethane distribution. Deep-Sea Research 34, 1957–1980.
Walsh, D., Carmack, E.C., 2002. Evanescent behavior of Arctic intrusions. Journal of Marine Research 60, 281–310.
Walsh, D., Carmack, E.C., 2003. The nested thermohaline structure of Arctic intrusions. Ocean Modelling 5, 267–289.
Weingartner, T., Aagaard, K., Woodgate, R., Danielson, S., Sasaki, Y., Cavalieri, D., 2005. Circulation on the north central Chukchi sea shelf. Deep-Sea Research. II 52 (24–26), 3150–3174.
Woodgate, R.A., Aagaard, K., Muench, R.D., Gunn, J., Björk, G., Rudels, B., Roach, A.T., Schauer, U., 2001. The Arctic Ocean boundary current along the Eurasian slope and the adjacent Lomonosov Ridge: water mass properties, transports and transformations from moored instruments. Deep-Sea Research I 48, 1757–1792.
Woodgate, R.A., Aagaard, K., Swift, J.H., Falkner, K.K., Smethie Jr., W.M., 2005a. Pacific ventilation of the Arctic Ocean's lower halocline by upwelling and diapycnal mixing over the continental margin. Geophysical Research Letters 32 (18), L18609.
Woodgate, R.A., Aagaard, K., Weingartner, T., 2005b. A year in the physical oceanography of the Chukchi Sea: moored measurements from autumn 1990–1991. Deep-Sea Research II 52 (24–26), 3116–3149.
Woodgate, R.A., Aagaard, K., Swift, J.H., Smethie, W.M., Falkner, K.K., 2007. Atlantic water circulation over the Mendeleev Ridge and Chukchi Borderland from thermohaline intrusions and water mass properties. Journal of Geophysical Research 112, C02005.